AN AUTOMATED MULTILEVEL SUBSTRUCTURING METHOD FOR EIGENSPACE COMPUTATION IN LINEAR ELASTODYNAMICS

JEFFREY K. BENNIGHOF* AND R. B. LEHOUCQ†

Abstract. We present an automated multilevel substructuring (AMLS) method for eigenvalue computations in linear elastodynamics in a variational and algebraic setting. AMLS first recursively partitions the domain of the PDE into a hierarchy of subdomains. Then AMLS recursively generates a subspace for approximating the eigenvectors associated with the smallest eigenvalues by computing partial eigensolutions associated with the subdomains and the interfaces between them. We remark that although we present AMLS for linear elastodynamics, our formulation is abstract and applies to generic H^1-elliptic bilinear forms.

In the variational formulation, we define an interface mass operator that is consistent with the treatment of elastic properties by the familiar Steklov-Poincaré operator. With this interface mass operator, all of the subdomain and interface eigenvalue problems in AMLS become orthogonal projections of the global eigenvalue problem onto a hierarchy of subspaces. Convergence of AMLS is determined in the continuous setting by the truncation of these eigenspaces, independent of other discretization schemes.

The goal of AMLS, in the algebraic setting, is to achieve a high level of dimensional reduction, locally and inexpensively, while balancing the errors associated with truncation and the finite element discretization. This is accomplished by matching the mesh-independent AMLS truncation error with the finite element discretization error. Our report ends with numerical experiments that demonstrate the effectiveness of AMLS on a model and an industrial problem.

Key words. Eigenvalues, modal analysis, multilevel, substructuring, domain decomposition, dimensional reduction, finite elements, frequency response

AMS subject classifications. 65F15, 65N25, 65N30, 65N22, 65M60, 65N55, 65M55

1. Introduction.

Dynamic analysis of structures frequently involves finite element discretizations with over one million unknowns. One discretization is typically used for many solutions, such as in a harmonic response analysis at many frequencies, so that a dimensional reduction step is advantageous or even necessary. The standard reduction approach is modal truncation, which requires a costly partial eigensolution but reduces the number of unknowns by orders of magnitude. The approach used in industry for this partial eigensolution is the shift-invert block Lanczos [7] algorithm. The computational bottleneck of the algorithm is the linear set of equations that must be solved at every Lanczos iteration.

Modal truncation is justified in the continuous setting because higher eigenfunctions have much lower participation in the response than lower ones. But there is an additional justification when a finite element discretization is used. If a sufficient number of modes are retained, then the error associated with modal truncation is of the same order as the discretization error. The implication is that the cost of the harmonic response may be dramatically reduced without a significant loss of accuracy.

The cost of the partial eigensolution required for modal truncation may substantially increase as the frequency range for the analysis increases. This is because the

*Department of Aerospace Engineering & Engineering Mechanics, The University of Texas at Austin, Austin, TX 78712-1085 bennighof@mail.utexas.edu.

†Sandia National Laboratories, P.O. Box 5800, MS 1110, Albuquerque, NM 87185-1110 rblehou@sandia.gov. Sandia is a multiprogram laboratory operated by Sandia Corporation, a Lockheed Martin Company, for the United States Department of Energy under Contract DE-AC04-94AL85000.

number of eigenvectors needed can easily reach into the thousands. High modal density (close spacing of eigenvalues) also contributes to the cost. An alternative to this approach is the automated multilevel substructuring (AMLS) method, in which the structure is recursively divided into thousands of subdomains. Eigenvectors associated with these subdomains are used to represent the structure's response, rather than the traditional global eigenvectors. Dimensional reduction of the finite element discretization is based on many small, local, and inexpensive eigenvalue problems and so any costly linear solves with the global mass and stiffness matrices are avoided.

Before we continue with our introduction, we motivate the relevance of AMLS via a recently accomplished calculation that demonstrates its impact within the structural dynamics community. Recently, Kropp and Heiserer [12] benchmarked the commercial implementation of AMLS[1] against the industry standard shift-invert block Lanczos [7] algorithm available in MSC.Nastran within a vibro-acoustic analysis. Their report concludes that the use of AMLS allows BMW to double the frequency range of interest with commodity workstations in an order of magnitude less computing time than the standard approach on a CRAY SV1 supercomputer. Moreover, they describe a calculation where nearly $2,500$ eigenvectors were computed for a matrix pencil of order just over $13,500,000$ performed on a HP-RISC workstation; this eigenanalysis was infeasible on the CRAY SV1 with the Lanczos algorithm. The authors are not aware of any similar calculation let alone one computed on a workstation. We anticipate that our report will provide a description of AMLS and so assist the development and implementation of modal truncation methods needed to solve the next generation of large-scale problems in structural dynamics.

The goal of our report is to carefully describe the mathematical basis for AMLS in the continuous variational setting and relationship to the algebraic formulation. We describe how differential eigenvalue problems are defined on subdomains and on interfaces between subdomains. For the interface eigenvalue problems, an operator is defined that acts on interface trace functions and consistently represents mass associated with extensions of these trace functions. All of these differential eigenvalue problems are then shown to be projections of the global eigenvalue problem onto a hierarchy of orthogonal subspaces. The eigenfunctions of these problems are orthogonal with respect to the energy inner product and generate a basis for the space of admissible functions on the global domain. We remark that although we present AMLS for linear elastodynamics, our formulation is abstract and applies to generic H^1-elliptic bilinear forms.

AMLS is a generalization of classical component mode synthesis (CMS) techniques [9, 6] (see [15] for a recent review of component mode synthesis methods). In particular, our variational formulation is a multilevel extension of work by Bourquin, and Bourquin and d'Hennezel [2, 3, 5, 4] that contains the first mathematical analysis of CMS. In addition to the variational multilevel extension, we prove that AMLS is a congruence transformation that arises from a matrix decomposition of the stiffness matrix. The congruence transformation is carefully linked to the variational formulation of AMLS. This congruence transformation allows us to treat AMLS as a purely algebraic process; this is new work and motivates a high-performance implementation. Our third contribution is our treatment of the interface eigenvalue problem; as described in the previous paragraph, AMLS uses a consistent treatment of mass in contrast to the approach suggested by Bourquin. Finally, we are not aware of any other research on multilevel substructuring for elliptic PDE eigenvalue problems and

[1] CDH/AMLS (www.cdh-gmbh.com)

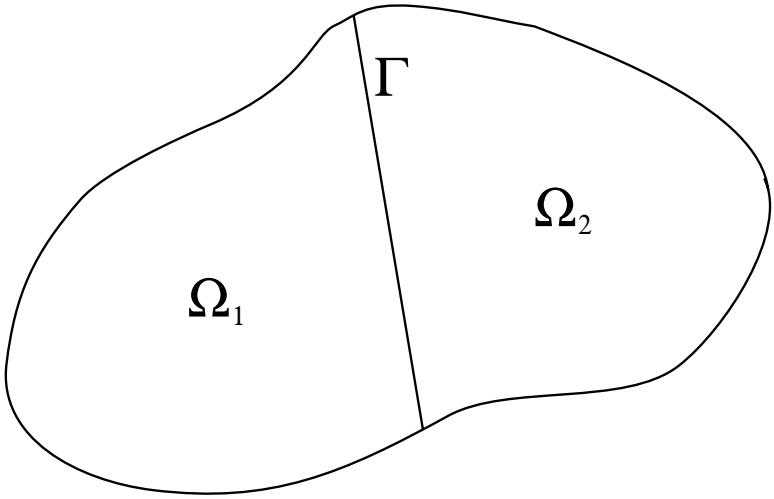

FIG. 2.1. *The domain Ω partitioned two subdomains along an interface Γ.*

the breakthrough calculation in the paper by Kropp and Heiserer [12] achieved by AMLS justifies a careful description of the underlying algorithm.

When AMLS is applied to a finite element discretization, the error in approximating the global eigensolution is associated with both the finite element approximation and truncation of the subdomain eigensolutions. For AMLS, convergence depends on modal truncation and is independent of mesh size for a conforming finite element method. This suggests that AMLS is a scalable approach for large problems. The objective of our dimensional reduction is to retain only as many subdomain eigenvectors as are needed so that the eigenspace truncation and finite element discretization errors are consistent. This is an attractive alternative to the standard practice of computing a costly partial eigensolution for an extremely large matrix pencil.

Our report is organized as follows. We present a single-level application of AMLS in a continuous variational formulation in §2. We then present the single-level method in §3 in the discrete setting resulting from a finite element discretization. These first two sections introduce AMLS in the simplest possible setting. Section 4 is the heart of the report extending the results of §2–3 to the multilevel case. Our report concludes with numerical experiments applying AMLS to a simple model problem and to a large industrial problem in §5.

We quickly review our use of standard notation. Let Ω be a two or three dimensional domain with Lipschitz boundary $\partial\Omega$ and so let $H^1(\Omega)$ denote a Sobolev space of order 1; $H_0^1(\Omega)$ denote a subspace of $H^1(\Omega)$ consisting of functions that vanish on $\partial\Omega$; $H_{00}^{1/2}(\Gamma)$ denote the trace space of $H_0^1(\Omega)$ on Γ; and let the dual spaces of $H_0^1(\Omega)$ and $H_{00}^{1/2}(\Gamma)$ be denoted by $H^{-1}(\Omega)$ and $H^{-1/2}(\Gamma)$, respectively. Let the norms and inner products on $H^1(\Omega)$ be given by $\|\cdot\|_1$ and $(\cdot,\cdot)_1$, respectively; and let $\langle\cdot,\cdot\rangle$ denote the duality pairing between a subspace and its dual.

2. Single-level method: Continuous setting. In this section, we present a single-level scheme for generating an approximating subspace in a continuous setting, leaving the generalization to the more rewarding multilevel approach for §4. In this approach, eigenvalue problems are used to generate components of the subspace. This method is a generalization of classical component mode synthesis techniques.

The scheme is presented here in the context of the differential eigenvalue problem in elastodynamics.

The differential eigenvalue problem associated with the free vibration of an elastic solid has the form

$$\begin{cases} -\operatorname{div}\sigma(u) = \lambda\rho u & \text{in } \Omega \\ u = 0 & \text{on } \partial\Omega, \end{cases}$$

where the eigenvalue λ is the square of the natural frequency $2\pi\omega$ and ρ is the mass density. We remark that Dirichlet boundary conditions are used here for simplicity, but the method is not limited to this choice of boundary conditions. Here, $\sigma(u)$ is the linearized stress tensor associated with the displacement u, obtained from the inner product between the fourth-order tensor of elastic coefficients $\mathcal{C}_{ijkl}$ and the linearized strain tensor

$$\epsilon_{kl}(u) = \frac{1}{2}\left(\frac{\partial u_k}{\partial x_l} + \frac{\partial u_l}{\partial x_k}\right).$$

In variational form, the differential eigenvalue problem can be expressed as: Find $(u,\lambda) \in H_0^1(\Omega) \times \mathbb{R}$ such that

$$a(u,v) = \lambda\, b(u,v) \quad \forall v \in H_0^1(\Omega), \tag{2.1}$$

where $H_0^1(\Omega)$ is the space of admissible functions and the bilinear forms

$$a(u,v) = \int_\Omega \sum_{i,j} \sigma_{ij}(u)\epsilon_{ij}(v)\, d\Omega \quad \text{and} \quad b(u,v) = \int_\Omega \rho uv\, d\Omega \tag{2.2}$$

are associated with elastic and inertial properties, respectively. We will refer to (2.1) as the global eigenvalue problem. Straightforward arguments show that $a(\cdot,\cdot)$ and $b(\cdot,\cdot)$ are coercive symmetric bilinear forms, implying that the eigenvalues are positive and the eigenvectors are orthogonal with respect to some inner product.

We partition the domain Ω into two subdomains Ω_1 and Ω_2 that share the interface $\Gamma = \overline{\Omega}_1 \cap \overline{\Omega}_2$. See Figure 2.1 for an example domain. We denote the outward normal unit vector for subdomain Ω_i on Γ by η_i. The remainder of this section explains how the global eigenvalue problem is orthogonally projected onto subspaces associated with Ω_1, Ω_2 and Γ. The resulting eigenfunctions of these three eigenvalue problems define a set of trial functions for solving the global eigenvalue problem.

For the subdomains Ω_i, $i = 1, 2$, we define subspaces of functions that are nonzero in Ω_i and are trivially extended throughout Ω as

$$V_{\Omega_i} = \{v \in H_0^1(\Omega) \colon v|_{\Omega\setminus\Omega_i} = 0\}, \tag{2.3}$$

and solve the two *fixed-interface* eigenvalue problems: Find $(u,\lambda) \in V_{\Omega_i} \times \mathbb{R}$ such that

$$a(u,v) = \lambda\, b(u,v) \quad \forall v \in V_{\Omega_i}. \tag{2.4}$$

In words, we solve two subdomain eigenvalue problems that are subject to Dirichlet boundary conditions on both the boundary $\partial\Omega$ of the global domain and the interface Γ.

For the eigenvalue problem associated with the interface Γ, we first define the extension of a trace function that is defined on Γ. The extension $v \in H_0^1(\Omega)$ of a trace function $\tau \in H_{00}^{1/2}(\Gamma)$ solves the minimization problem

$$\inf_{v \in H_0^1(\Omega)} a(v,v) \quad \text{subject to} \quad v|_\Gamma = \tau.$$

We denote the unique extension that solves this minimization problem as $E_\Omega \tau = v$. In an analogous fashion, we define the subdomain extension operator E_{Ω_i} by $E_{\Omega_i}\tau = (E_\Omega \tau)|_{\Omega_i}$ and a subspace of extensions of trace functions by

$$V_\Gamma = \{E_\Omega v \colon v \in H_{00}^{1/2}(\Gamma)\}. \tag{2.5}$$

We will make use of the following well-known result, whose proof follows from applying elementary variational techniques to the minimization problem.

LEMMA 2.1. *Let $a(\cdot,\cdot)$, V_{Ω_i} and V_Γ be as defined in (2.2), (2.3) and (2.5). If $u \in V_{\Omega_i}$ and $v \in V_\Gamma$, then $a(u,v) = 0$.*

The *coupling mode* eigenvalue problem associated with the interface Γ is: Find $(u,\lambda) \in V_\Gamma \times \mathbb{R}$ such that

$$a(u,v) = \lambda b(u,v) \quad \forall v \in V_\Gamma.$$

Note that the only differences between this problem and (2.4) are the subspaces containing u and v. Because an element of V_Γ is determined by its trace on Γ, this eigenvalue problem can be equivalently expressed as: Find $(u,\lambda) \in H_{00}^{1/2}(\Gamma) \times \mathbb{R}$ such that

$$a(E_\Omega u, E_\Omega v) = \lambda b(E_\Omega u, E_\Omega v) \quad \forall v \in H_{00}^{1/2}(\Gamma). \tag{2.6}$$

The following theorem establishes that the two fixed interface and coupling mode eigenvalue problems represent the orthogonal projections of the global eigenvalue problem onto the subspaces V_{Ω_1}, V_{Ω_2} and V_Γ.

THEOREM 2.2. *If V_{Ω_i}, V_Γ and $a(\cdot,\cdot)$ are defined as above, then the direct sum*

$$V_{\Omega_1} \oplus V_{\Omega_2} \oplus V_\Gamma$$

is an orthogonal decomposition of $H_0^1(\Omega)$ in the inner product defined by $a(\cdot,\cdot)$.

Proof. For $u \in H_0^1(\Omega)$ define the projections onto V_Γ and V_{Ω_i} as $\mathcal{P}_{\Gamma_i} u = E_\Omega(u|_\Gamma)$ and $\mathcal{P}_{\Omega_i} u = (u - \mathcal{P}_\Gamma u)|_{\Omega_i}$. Lemma 2.1 shows that $a(\mathcal{P}_{\Omega_i} u, \mathcal{P}_\Gamma u) = 0$ and the theorem is proved. ∎

We now define the bilinear forms of the coupling mode eigenvalue problem in terms of operators acting on trace functions. We first note that

$$a(E_\Omega u, E_\Omega v) = \langle \mathcal{S} u, v \rangle \quad \forall u, v \in H_{00}^{1/2}(\Gamma),$$

where $\mathcal{S}$ is the well-known Steklov-Poincaré operator (see [14]) expressed in strong form for our elasticity problem by

$$\mathcal{S}\tau = \sum_{i=1}^{2} (\sigma(E_{\Omega_i}\tau) \cdot \eta_i)|_\Gamma, \tag{2.7}$$

where $\tau \in H_{00}^{1/2}(\Gamma)$. We also need a mass operator $\mathcal{M}$ so that

$$b(E_\Omega u, E_\Omega v) = \langle \mathcal{M} u, v \rangle \quad \forall u, v \in H_{00}^{1/2}(\Gamma),$$

and hence the representation of inertial properties is consistent with the representation of elastic properties. Such a mass operator is given, in strong form, by

$$\mathcal{M}\tau = \sum_{i=1}^{2} -(\sigma(\mathcal{G}_i(\rho E_{\Omega_i}\tau)) \cdot \eta_i)|_\Gamma, \tag{2.8}$$

where the Green's function for the Dirichlet elasticity problem on subdomain Ω_i is defined by: Find $\mathcal{G}_i(f) \in V_{\Omega_i}$ such that

$$a(\mathcal{G}_i(f), v) = \langle f, v\rangle \in H^{-1}(\Omega) \quad \forall v \in V_{\Omega_i}.$$

This mass operator $\mathcal{M}$ represents an extension of a trace function, multiplication by ρ, and reduction back to the interface. Mechanically, the reduction step treats the function $\rho E_{\Omega_i}\tau$ as a load and finds the corresponding displacement via the Green's function, and then the normal component of stress associated with this displacement is evaluated at the interface. This stress component acts as a surface traction on each of the subdomains.

The following theorem summarizes our discussion above and presents the coupling mode eigenvalue problem in terms of operators acting on trace functions.

THEOREM 2.3. *The coupling mode eigenvalue problem (2.6) is equivalent to the eigenvalue problem: Find* $(u, \lambda) \in H_{00}^{1/2}(\Gamma) \times \mathbb{R}$ *such that*

$$\langle \mathcal{S}u, v\rangle = \lambda\langle \mathcal{M}u, v\rangle \quad \forall v \in H_{00}^{1/2}(\Gamma).$$

Proof. Green's formula gives

$$\begin{aligned} b(E_\Omega u, E_\Omega v) &= \sum_{i=1}^{2} \int_{\Omega_i} \rho(E_{\Omega_i} u)(E_{\Omega_i} v)\, d\Omega_i \\ &= \sum_{i=1}^{2} a(\mathcal{G}_i(\rho E_{\Omega_i} u), E_{\Omega_i} v) - \int_\Gamma (\sigma(\mathcal{G}_i(\rho E_{\Omega_i} u)) \cdot \eta_i)|_\Gamma E_{\Omega_i} v|_\Gamma \, d\Gamma. \end{aligned}$$

The integration over Γ results because $E_\Omega v$ has a nonzero trace on Γ. Lemma 2.1 implies that $a(\mathcal{G}_i(\rho E_{\Omega_i} u), E_{\Omega_i} v) = 0$ and so $b(E_\Omega u, E_\Omega v) = \langle \mathcal{M}u, v\rangle$, and the theorem is proved. ∎

We remark that the coupling mode eigenvalue problem of the theorem resembles the one proposed by Bourquin and d'Hennezel, who also solved an eigenvalue problem on the interface to obtain *coupling modes*. However, their interface eigenvalue problem did not use the consistent mass operator $\mathcal{M}$. Instead, they solved for eigenfunctions of the Steklov-Poincaré operator, or optionally included the mass density ρ, evaluated along Γ, in the right-hand side of the interface eigenvalue problem.

When the operator $\mathcal{M}$ is used, the coupling mode eigenvalue problem is a projection of the global eigenvalue problem onto the subspace of extensions V_Γ. At first glance, this distinction is innocuous enough; however, this consistent projection of the inertial term to the interface is of fundamental importance. The result is that a consistent truncation of eigenvalues for fixed-interface and coupling mode eigenvalue problems is possible. This consistency is vital in the multilevel case, for which the truncation issue is more involved.

3. Single-level method: Finite element discretization and algebraic setting. A finite element discretization of (2.1) results in the global algebraic eigenvalue problem

$$\mathbf{K}\boldsymbol{\phi} = \lambda^h \mathbf{M}\boldsymbol{\phi} \tag{3.1}$$

where $\mathbf{K}$ and $\mathbf{M}$ are stiffness and mass matrices of order n. The remainder of this section demonstrates that AMLS is a matrix decomposition.

One-way dissection on the union of the graphs of the mass and stiffness matrices reorders $\mathbf{K}$ and $\mathbf{M}$ into

$$\begin{bmatrix} \mathbf{K}_{\Omega_1} & 0 & \mathbf{K}_{\Omega_1,\Gamma} \\ 0 & \mathbf{K}_{\Omega_2} & \mathbf{K}_{\Omega_2,\Gamma} \\ \mathbf{K}_{\Omega_1,\Gamma}^T & \mathbf{K}_{\Omega_2,\Gamma}^T & \mathbf{K}_{\Gamma} \end{bmatrix} \quad \text{and} \quad \begin{bmatrix} \mathbf{M}_{\Omega_1} & 0 & \mathbf{M}_{\Omega_1,\Gamma} \\ 0 & \mathbf{M}_{\Omega_2} & \mathbf{M}_{\Omega_2,\Gamma} \\ \mathbf{M}_{\Omega_1,\Gamma}^T & \mathbf{M}_{\Omega_2,\Gamma}^T & \mathbf{M}_{\Gamma} \end{bmatrix}. \tag{3.2}$$

The unknowns associated with rows and columns identified by Γ constitute a separator for the graph. The finite element nodes associated with this separator identify element boundaries that form the interface Γ. The entries in the Γ rows and columns in $\mathbf{K}$ and $\mathbf{M}$ are obtained by integrating over the elements adjacent to the interface Γ. The submatrices $\mathbf{K}_{\Omega_i}$ and $\mathbf{M}_{\Omega_i}$ are associated with the interiors of subdomains Ω_i and are of order n_{Ω_i}. We denote the order of $\mathbf{K}_\Gamma$ by n_Γ. Submatrices $\mathbf{K}_{\Omega_i,\Gamma}$ and $\mathbf{M}_{\Omega_i,\Gamma}$ for $i = 1, 2$ represent coupling between subdomain interior unknowns and unknowns at the interface. We remark that under mild conditions, graph partitioning software [8, 11] algebraically computes a separator that results in two physically separated subdomains.

Block Gaussian elimination on $\mathbf{K}$ results in $\mathbf{U}^T\mathbf{K}\mathbf{U} = \text{diag}[\ \mathbf{K}_{\Omega_1} \quad \mathbf{K}_{\Omega_2} \quad \tilde{\mathbf{K}}_\Gamma\ ]$ where

$$\mathbf{U} = \begin{bmatrix} \mathbf{I}_{n_{\Omega_1}} & 0 & -\mathbf{K}_{\Omega_1}^{-1}\mathbf{K}_{\Omega_1,\Gamma} \\ 0 & \mathbf{I}_{n_{\Omega_2}} & -\mathbf{K}_{\Omega_2}^{-1}\mathbf{K}_{\Omega_2,\Gamma} \\ 0 & 0 & \mathbf{I}_{n_\Gamma} \end{bmatrix}. \tag{3.3}$$

The matrix

$$\tilde{\mathbf{K}}_\Gamma = \mathbf{K}_\Gamma - \sum_{i=1}^{2} \mathbf{K}_{\Omega_i,\Gamma}^T \mathbf{K}_{\Omega_i}^{-1} \mathbf{K}_{\Omega_i,\Gamma}$$

is the Schur complement of $\text{diag}[\ \mathbf{K}_{\Omega_1} \quad \mathbf{K}_{\Omega_2}\ ]$ in $\mathbf{K}$, and is the discrete equivalent of the Steklov-Poincaré operator (2.7). If we perform a congruence transformation on (3.1) with $\mathbf{U}$, then we obtain

$$\mathbf{U}^T\mathbf{K}\mathbf{U}\tilde{\boldsymbol{\phi}} = \text{diag}[\ \mathbf{K}_{\Omega_1} \quad \mathbf{K}_{\Omega_2} \quad \tilde{\mathbf{K}}_\Gamma\ ]\tilde{\boldsymbol{\phi}} = \mathbf{U}^T\mathbf{M}\mathbf{U}\tilde{\boldsymbol{\phi}}\lambda_h \tag{3.4}$$

where $\boldsymbol{\phi} = \mathbf{U}\tilde{\boldsymbol{\phi}}$ and the upper triangular part of the symmetric matrix $\mathbf{U}^T\mathbf{M}\mathbf{U}$ is

$$\begin{bmatrix} \mathbf{M}_{\Omega_1} & \mathbf{0} & \mathbf{M}_{\Omega_1,\Gamma} - \mathbf{M}_{\Omega_1}\mathbf{K}_{\Omega_1}^{-1}\mathbf{K}_{\Omega_1,\Gamma} \\ \mathbf{0} & \mathbf{M}_{\Omega_2} & \mathbf{M}_{\Omega_2,\Gamma} - \mathbf{M}_{\Omega_2}\mathbf{K}_{\Omega_2}^{-1}\mathbf{K}_{\Omega_2,\Gamma} \\ \star & \star & \tilde{\mathbf{M}}_\Gamma \end{bmatrix}. \tag{3.5}$$

The matrix $\tilde{\mathbf{M}}_\Gamma$ is

$$\mathbf{M}_\Gamma - \sum_{i=1}^{2} \left(\mathbf{K}_{\Omega_i,\Gamma}^T \mathbf{K}_{\Omega_i}^{-1} \mathbf{M}_{\Omega_i,\Gamma} + \mathbf{M}_{\Omega_i,\Gamma}^T \mathbf{K}_{\Omega_i}^{-1} \mathbf{K}_{\Omega_i,\Gamma} - \mathbf{K}_{\Omega_i,\Gamma}^T \mathbf{K}_{\Omega_i}^{-1} \mathbf{M}_{\Omega_i} \mathbf{K}_{\Omega_i}^{-1} \mathbf{K}_{\Omega_i,\Gamma}\right)$$

and is the discrete version of the mass complement operator (2.8).

The eigendecompositions associated with the fixed-interface and coupling mode problems are

$$\mathbf{K}_{\Omega_i}\mathbf{Z}_{\Omega_i,} = \mathbf{M}_{\Omega_i}\mathbf{Z}_{\Omega_i,}\boldsymbol{\Lambda}_{\Omega_i} \quad \text{and} \quad \tilde{\mathbf{K}}_\Gamma\mathbf{Z}_\Gamma = \tilde{\mathbf{M}}_\Gamma\mathbf{Z}_\Gamma\boldsymbol{\Lambda}_\Gamma$$

where we assume that $\mathbf{Z}_{\Omega_i,}^T \mathbf{M}_{\Omega_i} \mathbf{Z}_{\Omega_i,} = \mathbf{I}_{n_{\Omega_i}}$ and $\mathbf{Z}_\Gamma^T \tilde{\mathbf{M}}_\Gamma \mathbf{Z}_\Gamma = \mathbf{I}_{n_\Gamma}$. If we define the matrix

$$\mathbf{Z} = \text{diag}[\ \mathbf{Z}_{\Omega_1} \quad \mathbf{Z}_{\Omega_2} \quad \mathbf{Z}_\Gamma\ ] \tag{3.6}$$

then

$$(\mathbf{UZ})^T \mathbf{K}(\mathbf{UZ}) = \mathbf{D} = \text{diag}[\ \mathbf{\Lambda}_1 \quad \mathbf{\Lambda}_2 \quad \mathbf{\Lambda}_\Gamma\ ] \tag{3.7}$$

and

$$(\mathbf{UZ})^T \mathbf{M}(\mathbf{UZ}) = \begin{bmatrix} \mathbf{I}_{n_{\Omega_1}} & \mathbf{0} & \mathbf{Z}_{\Omega_1}^T(\mathbf{M}_{\Omega_1,\Gamma} - \mathbf{M}_{\Omega_1}\mathbf{K}_{\Omega_1}^{-1}\mathbf{K}_{\Omega_1,\Gamma})\mathbf{Z}_\Gamma \\ \mathbf{0} & \mathbf{I}_{n_{\Omega_2}} & \mathbf{Z}_{\Omega_2}^T(\mathbf{M}_{\Omega_2,\Gamma} - \mathbf{M}_{\Omega_2}\mathbf{K}_{\Omega_2}^{-1}\mathbf{K}_{\Omega_2,\Gamma})\mathbf{Z}_\Gamma \\ \star & \star & \mathbf{I}_{n_\Gamma} \end{bmatrix}. \tag{3.8}$$

Although we can solve the eigenvalue problem

$$(\mathbf{UZ})^T \mathbf{K}(\mathbf{UZ})\mathbf{v} = (\mathbf{UZ})^T \mathbf{M}(\mathbf{UZ})\mathbf{v}\lambda^h \tag{3.9}$$

where $\boldsymbol{\phi} = \mathbf{UZv}$ to determine the global eigenvectors, we instead perform a modal truncation on the fixed-interface and coupling mode eigenvalue problems. Let $\mathbf{R}_{\Omega_i}$ and $\mathbf{R}_\Gamma$ be submatrices of $\mathbf{I}_{n_{\Omega_i}}$ and $\mathbf{I}_{n_\Gamma}$ with n_{Ω_i} and n_Γ rows so that $m_{\Omega_i} < n_{\Omega_i}$ and $m_\Gamma < n_\Gamma$ columns. Moreover, $\mathbf{R}_{\Omega_i}$ and $\mathbf{R}_\Gamma$ are selected so that $\mathbf{R}_{\Omega_i}^T \mathbf{\Lambda}_{\Omega_i} \mathbf{R}_{\Omega_i}$ and $\mathbf{R}_\Gamma^T \mathbf{\Lambda}_\Gamma \mathbf{R}_\Gamma$ retain only the smallest eigenvalues (say those within some frequency range of interest) associated with Ω_i and Γ. Denote by

$$\mathbf{R} = \text{diag}[\ \mathbf{R}_{\Omega_1} \quad \mathbf{R}_{\Omega_2} \quad \mathbf{R}_\Gamma\ ] \tag{3.10}$$

the block diagonal restriction matrix with $n_{\Omega_1} + n_{\Omega_2} + n_\Gamma$ and $m_{\Omega_1} + m_{\Omega_2} + m_\Gamma$ rows and columns, respectively. The preceding discussion has proved the following lemma.

LEMMA 3.1. *Let* $\mathbf{U}$, $\mathbf{Z}$, $\mathbf{\Lambda}$ *and* $\mathbf{R}$ *be as defined in (3.3),(3.6) and (3.10). If* $\hat{\mathbf{D}} = (\mathbf{UZR})^T \mathbf{K}(\mathbf{UZR})$ *and* $\hat{\mathbf{M}} = (\mathbf{UZR})^T \mathbf{M}(\mathbf{UZR})$ *then*

$$\hat{\mathbf{D}}\mathbf{x} = \lambda^{m,h} \hat{\mathbf{M}}\mathbf{x} \tag{3.11}$$

is an eigenvalue problem of order $m = m_{\Omega_1} + m_{\Omega_2} + m_\Gamma$ *where* $(\mathbf{UZR})\mathbf{x}$ *is an approximation to an eigenvector* $\boldsymbol{\phi}$ *of (3.1).*

We identify $\hat{\mathbf{D}}$ and $\hat{\mathbf{M}}$ as *coarse* approximations to the stiffness and mass matrices. The lemma demonstrates that eigenvectors for (3.1) are approximated by computing a partial eigensolution of the two fixed-interface and the coupling mode eigenvalue problems and then performing a Rayleigh-Ritz analysis (3.11). The order of the eigenvalue problem (3.11) is $m_{\Omega_1} + m_{\Omega_2} + m_\Gamma$ and is typically significantly smaller than n. The error of the eigenfunction approximations is associated with both the finite element discretization and the truncation of the coupling and fixed interface eigenvalue problems. We refer the interested reader to [5], where error bounds appear that account for both sources of error.

4. Continuous and Discrete Multilevel Application. This section generalizes the results of the previous two sections to a multilevel formulation of the method where we recursively subdivide subdomains Ω_1 and Ω_2 to additional levels. The multilevel case calls for a modification of notation.

We denote the j-th subdomain on level i by $\Omega_{i,j}$, beginning with the global domain $\Omega = \Omega_{0,1}$. Each subdomain $\Omega_{i,j}$ is further partitioned into subdomains on level $i+1$

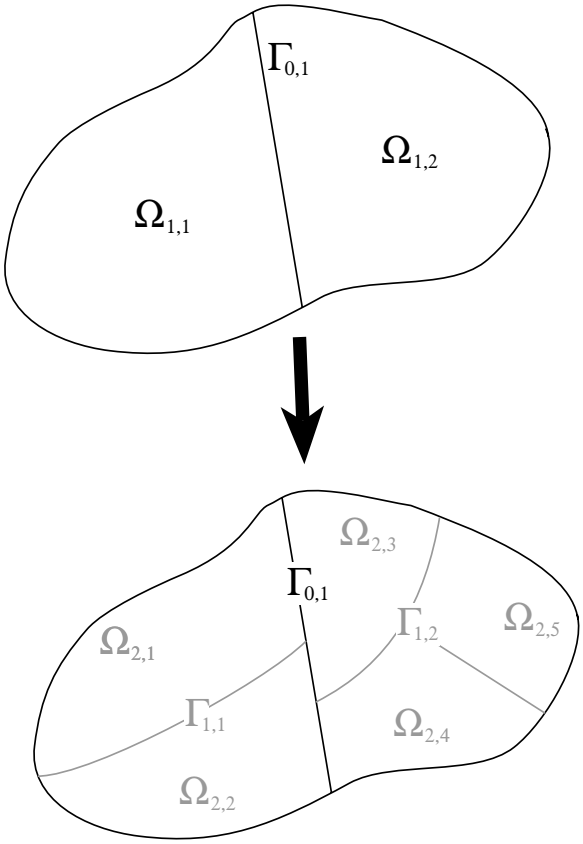

FIG. 4.1. *Two level partitioning of* $\Omega = \Omega_{0,1}$*;* $\ell = 2$*,* $s_0 = 1$*,* $s_1 = 2$ *and* $s_2 = 5$*.*

by the interface(s) constituting $\Gamma_{i,j}$. The total number of subdomains on level i is s_i. Such a multilevel partitioning can be represented as a tree, with $\Omega_{0,1}$ at the root and $\Omega_{\ell,j}$ at the leaves. We assume for simplicity that all of the leaf subdomains in the subdomain tree are on level ℓ, which means that all subdomains in any branch of the tree are recursively subdivided until level ℓ is reached. We refer to all nodes of the tree as substructures but note that only the substructures at the leaf level correspond to $\Omega_{\ell,j}$ (fixed interface problems) and the remainder of the substructures correspond to interfaces $\Gamma_{i,j}$ (coupling mode problems). Figures 4.1 and 4.2 illustrate the partitioned domain and corresponding tree when $\ell = 2$, $s_0 = 1$, $s_1 = 2$ and $s_2 = 5$.

Let $E^{i,j}\tau$ be the energy minimizing extension of $\tau \in H_{00}^{1/2}(\Gamma_{i,j})$ into $\Omega_{i,j}$ that is zero on $\Omega/\Omega_{i,j}$. Then $E^{i,j}\tau$ is an element of the subspace

$$V_{E^{i,j}} = \{E^{i,j}\tau : \tau \in H_{00}^{1/2}(\Gamma_{i,j})\}.$$

Without loss of generality, we also let $E^{i,j}\tau$ denote the extension of τ into Ω that is zero on $\Omega/\Omega_{i,j}$. Define the subspace of extensions into subdomains on level i as

$$V_{E^i} = \bigoplus_{j=1}^{s_i} V_{E^{i,j}},$$

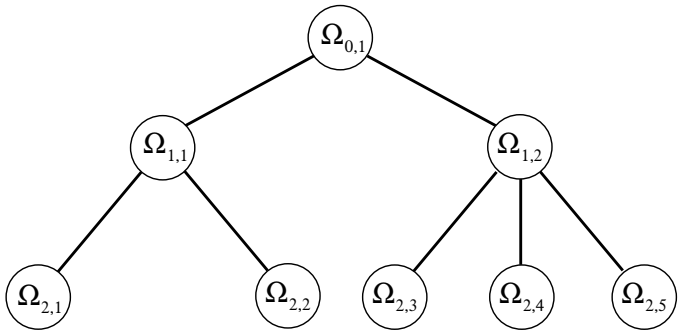

FIG. 4.2. *Tree associated with the two level domain partitioning;* $\ell = 2$, $s_0 = 1$, $s_1 = 2$ *and* $s_2 = 5$.

and the subspaces

$$V_{i,j} = \{v \in H_0^1(\Omega) : v|_{\Omega \setminus \Omega_{i,j}} = 0\}.$$

The following result is a generalization of Theorem 2.2 to a multilevel partitioning into subdomains.

THEOREM 4.1. *If the subspaces* $V_{i,j}$ *and* V_{E^i} *are defined as above, and* ℓ *is the level number for leaf subdomains in the subdomain tree, then*

$$H_0^1(\Omega) = \left(\bigoplus_{j=1}^{s_\ell} V_{\ell,j} \right) \oplus \left(\bigoplus_{j=0}^{\ell-1} V_{E^j} \right)$$

is an orthogonal decomposition in the bilinear form $a(\cdot, \cdot)$.

Proof. We prove the result using mathematical induction. A simple extension of Theorem 2.2 establishes the base case, which is that

$$H_0^1(\Omega) = \left(\bigoplus_{j=1}^{s_1} V_{1,j} \right) \oplus V_{E^0}$$

is such an orthogonal decomposition. Now let us suppose that

$$H_0^1(\Omega) = \left(\bigoplus_{j=1}^{s_i} V_{i,j} \right) \oplus \left(\bigoplus_{j=0}^{i-1} V_{E^j} \right) \tag{4.1}$$

is our inductive hypothesis and we will show that this decomposition holds for level $i+1$. If we subdivide a subdomain $\Omega_{i,j}$, then the orthogonal decomposition

$$V_{i,j} = \left(\bigoplus_{k \in \mathcal{I}_{i,j}} V_{i+1,k} \right) \oplus V_{E^{i,j}}$$

is also an application of Theorem 2.2, where $\mathcal{I}_{i,j} = \{k : \Omega_{i+1,k} \subset \Omega_{i,j}\}$ is the set of indices for subdomains on level $i+1$ that are contained in $\Omega_{i,j}$. The union of sets $\mathcal{I}_{i,j}$ over all subdomains $\Omega_{i,j}$ on level i is the set of all indices for subdomains on level

$i+1$. Therefore, we have the orthogonal decomposition

$$\begin{aligned}\bigoplus_{j=1}^{s_i} V_{i,j} &= \left(\bigoplus_{j=1}^{s_{i+1}} V_{i+1,j}\right) \oplus \left(\bigoplus_{j=1}^{s_i} V_{E^{i,j}}\right) \\ &= \left(\bigoplus_{j=1}^{s_{i+1}} V_{i+1,j}\right) \oplus V_{E^i}.\end{aligned}$$

Substituting this in the expression in (4.1) yields the result

$$H_0^1(\Omega) = \left(\bigoplus_{j=1}^{s_{i+1}} V_{i+1,j}\right) \oplus \left(\bigoplus_{j=0}^{i} V_{E^j}\right),$$

and the theorem is proved. □

The theorem implies that we need to solve s_ℓ fixed interface and $s_0 + \cdots + s_{\ell-1}$ coupling mode eigenvalue problems: Find $(u, \lambda) \in V_{\ell,j} \times \mathbb{R}$ such that

$$a(u, v) = \lambda\, b(u, v) \quad \forall v \in V_{\ell,j}, \;\; j = 1, \ldots, s_\ell;$$

and: Find $(u, \lambda) \in H_{00}^{1/2}(\Gamma_{i,k}) \times \mathbb{R}$ such that

$$\langle \mathcal{S}_{i,k} u, v\rangle = \lambda \langle \mathcal{M}_{i,k} u, v\rangle \quad \forall v \in H^{1/2}(\Gamma_{i,k}), \;\; i = 0, \ldots, \ell-1; k = 1, \ldots, s_i$$

where $\mathcal{S}_{i,k}$ and $\mathcal{M}_{i,k}$ are the Steklov-Poincaré and mass operators on $\Gamma_{i,k}$. Modal truncation can be performed on each of these eigenvalue problems.

However, in practice, as discussed in section 3, a finite element discretization of (2.1) leads to the discrete eigenvalue problem (3.1). A nested dissection ordering on the union of the graphs of the mass and stiffness matrices of (3.1) then provides a permutation of rows and columns that corresponds to a particular partitioning into subdomains. These reordered mass and stiffness matrices display a structure similar to (3.2) in which each fixed interface matrix also has the same structure to ℓ levels. The reordered stiffness and mass matrices contain s_ℓ blocks on the diagonal corresponding to subdomains on level ℓ, and $s_0 + \cdots + s_{\ell-1}$ blocks on the diagonal corresponding to interfaces. For example, Figure 4.3 illustrates the stiffness matrix corresponding to Figure 4.2. The mass matrix is analogously ordered. We remark that under mild conditions, graph partitioning software [8, 11] algebraically computes separators that results in physically separated subdomains.

Figure 4.3 illustrates that all of the blocks on the diagonal of the reordered $\mathbf{K}$ and $\mathbf{M}$ correspond either to terminal subdomains $\Omega_{\ell,j}$ in the tree, or to interfaces $\Gamma_{i,j}$ for $j = 1, \ldots, s_i$ on levels $i = 0, \ldots, \ell-1$. Denote by $\mathbf{U}_{\Gamma_{i,j}}$ the elementary block Gaussian eliminators designed to transform $\mathbf{K}$ to block diagonal form. For instance, Figure 4.4 displays the block Gaussian eliminators needed for the example of Figures 4.1 to 4.3 so that if $\mathbf{U}_1 \equiv \mathbf{U}_{\Gamma_{1,2}} \mathbf{U}_{\Gamma_{1,1}} \mathbf{U}_{\Gamma_{0,1}}$ then

$$\mathbf{U}_1^T \mathbf{K} \mathbf{U}_1 = \mathrm{diag}(\mathbf{K}_{\Omega_{2,1}}, \mathbf{K}_{\Omega_{2,2}}, \tilde{\mathbf{K}}_{\Gamma_{1,1}}, \mathbf{K}_{\Omega_{2,3}}, \mathbf{K}_{\Omega_{2,4}}, \mathbf{K}_{\Omega_{2,5}}, \tilde{\mathbf{K}}_{\Gamma_{1,2}} \tilde{\mathbf{K}}_{\Gamma_{0,1}}).$$

The mass matrix is also updated via a congruence transformation with $\mathbf{U}_1$ but is not rendered a block diagonal matrix. Instead $\mathbf{U}_1^T \mathbf{M} \mathbf{U}_1$ retains the block structure of $\mathbf{M}$. Note that the nontrivial block columns of $\mathbf{U}_{\Gamma_{i,j}}$ represent extension from $\Gamma_{i,j}$

$$\begin{bmatrix}
\mathbf{K}_{\Omega_{2,1}} & 0 & \mathbf{K}_{\Omega_{2,1},\Gamma_{1,1}} & 0 & 0 & 0 & 0 & \mathbf{K}_{\Omega_{2,1},\Gamma_{0,1}} \\
 & \mathbf{K}_{\Omega_{2,2}} & \mathbf{K}_{\Omega_{2,2},\Gamma_{1,1}} & 0 & 0 & 0 & 0 & \mathbf{K}_{\Omega_{2,2},\Gamma_{0,1}} \\
 & & \mathbf{K}_{\Gamma_{1,1}} & 0 & 0 & 0 & 0 & \mathbf{K}_{\Gamma_{1,1},\Gamma_{0,1}} \\
 & & & \mathbf{K}_{\Omega_{2,3}} & 0 & 0 & \mathbf{K}_{\Omega_{2,3},\Gamma_{1,2}} & \mathbf{K}_{\Omega_{2,3},\Gamma_{0,1}} \\
 & & & & \mathbf{K}_{\Omega_{2,4}} & 0 & \mathbf{K}_{\Omega_{2,4},\Gamma_{1,2}} & \mathbf{K}_{\Omega_{2,4},\Gamma_{0,1}} \\
 & & & & & \mathbf{K}_{\Omega_{2,5}} & \mathbf{K}_{\Omega_{2,5},\Gamma_{1,2}} & \mathbf{K}_{\Omega_{2,5},\Gamma_{0,1}} \\
 & & & & & & \mathbf{K}_{\Gamma_{1,2}} & \mathbf{K}_{\Gamma_{1,2},\Gamma_{0,1}} \\
 & & & & & & & \mathbf{K}_{\Gamma_{0,1}}
\end{bmatrix}$$

FIG. 4.3. *Two level substructuring; $\ell = 2$, $s_0 = 1$,$s_1 = 2$ and $s_2 = 5$; only the upper triangle of the symmetric stiffness matrix is displayed.*

$$\mathbf{U}_{\Gamma_{1,1}} = \begin{bmatrix}
\mathbf{I}_{n_{2,1}} & 0 & -\mathbf{K}_{\Omega_{2,1}}^{-1}\mathbf{K}_{\Omega_{2,1},\Gamma_{1,1}} & 0 & 0 & 0 & 0 & 0 \\
 & \mathbf{I}_{n_{2,2}} & -\mathbf{K}_{\Omega_{2,2}}^{-1}\mathbf{K}_{\Omega_{2,2},\Gamma_{1,1}} & 0 & 0 & 0 & 0 & 0 \\
 & & \mathbf{I}_{n_{1,1}} & 0 & 0 & 0 & 0 & 0 \\
 & & & \mathbf{I}_{n_{2,3}} & 0 & 0 & 0 & 0 \\
 & & & & \mathbf{I}_{n_{2,4}} & 0 & 0 & 0 \\
 & & & & & \mathbf{I}_{n_{2,5}} & 0 & 0 \\
 & & & & & & \mathbf{I}_{n_{1,2}} & 0 \\
 & & & & & & & \mathbf{I}_{n_{0,1}}
\end{bmatrix}$$

$$\mathbf{U}_{\Gamma_{1,2}} = \begin{bmatrix}
\mathbf{I}_{n_{2,1}} & 0 & 0 & 0 & 0 & 0 & 0 & 0 \\
 & \mathbf{I}_{n_{2,2}} & 0 & 0 & 0 & 0 & 0 & 0 \\
 & & \mathbf{I}_{n_{1,1}} & 0 & 0 & 0 & 0 & 0 \\
 & & & \mathbf{I}_{n_{2,3}} & 0 & 0 & -\mathbf{K}_{\Omega_{2,3}}^{-1}\mathbf{K}_{\Omega_{2,3},\Gamma_{1,2}} & 0 \\
 & & & & \mathbf{I}_{n_{2,4}} & 0 & -\mathbf{K}_{\Omega_{2,4}}^{-1}\mathbf{K}_{\Omega_{2,4},\Gamma_{1,2}} & 0 \\
 & & & & & \mathbf{I}_{n_{2,5}} & -\mathbf{K}_{\Omega_{2,5}}^{-1}\mathbf{K}_{\Omega_{2,5},\Gamma_{1,2}} & 0 \\
 & & & & & & \mathbf{I}_{n_{1,2}} & 0 \\
 & & & & & & & \mathbf{I}_{n_{0,1}}
\end{bmatrix}$$

$$\mathbf{U}_{\Gamma_{0,1}} = \begin{bmatrix}
\mathbf{I}_{n_{2,1}} & 0 & 0 & 0 & 0 & 0 & 0 & -\mathbf{K}_{\Omega_{2,1}}^{-1}\mathbf{K}_{\Omega_{2,1},\Gamma_{0,1}} \\
 & \mathbf{I}_{n_{2,2}} & 0 & 0 & 0 & 0 & 0 & -\mathbf{K}_{\Omega_{2,2}}^{-1}\mathbf{K}_{\Omega_{2,2},\Gamma_{0,1}} \\
 & & \mathbf{I}_{n_{1,1}} & 0 & 0 & 0 & 0 & -\tilde{\mathbf{K}}_{\Gamma_{1,1}}^{-1}\mathbf{K}_{\Gamma_{1,1},\Gamma_{0,1}} \\
 & & & \mathbf{I}_{n_{2,3}} & 0 & 0 & 0 & -\mathbf{K}_{\Omega_{2,3}}^{-1}\mathbf{K}_{\Omega_{2,3},\Gamma_{0,1}} \\
 & & & & \mathbf{I}_{n_{2,4}} & 0 & 0 & -\mathbf{K}_{\Omega_{2,4}}^{-1}\mathbf{K}_{\Omega_{2,4},\Gamma_{0,1}} \\
 & & & & & \mathbf{I}_{n_{2,5}} & 0 & -\mathbf{K}_{\Omega_{2,5}}^{-1}\mathbf{K}_{\Omega_{2,5},\Gamma_{0,1}} \\
 & & & & & & \mathbf{I}_{n_{1,2}} & -\tilde{\mathbf{K}}_{\Gamma_{1,2}}^{-1}\mathbf{K}_{\Gamma_{1,2},\Gamma_{0,1}} \\
 & & & & & & & \mathbf{I}_{n_{0,1}}
\end{bmatrix}$$

FIG. 4.4. *The three block Gaussian eliminators*

throughout subdomain $\Omega_{i,j}$ while the transpose of the same block column represents the reduction back to $\Gamma_{i,j}$.

In general, define

$$\mathbf{U}_{\ell-1} = (\Pi_{j=1}^{s_{\ell-1}}\mathbf{U}_{\Gamma_{\ell-1,j}})(\Pi_{j=1}^{s_{\ell-2}}\mathbf{U}_{\Gamma_{\ell-2,j}})\cdots\mathbf{U}_{\Gamma_{0,1}}. \tag{4.2}$$

$$\begin{bmatrix} -\mathbf{K}_{\Omega_{2,1}}^{-1}\mathbf{K}_{\Omega_{2,1},\Gamma_{0,1}} \\ -\mathbf{K}_{\Omega_{2,2}}^{-1}\mathbf{K}_{\Omega_{2,2},\Gamma_{0,1}} \\ 0 \\ 0 \\ 0 \\ 0 \\ 0 \\ \mathbf{I}_{n_{0,1}} \end{bmatrix} \quad \begin{bmatrix} 0 \\ 0 \\ 0 \\ -\mathbf{K}_{\Omega_{2,3}}^{-1}\mathbf{K}_{\Omega_{2,3},\Gamma_{0,1}} \\ -\mathbf{K}_{\Omega_{2,4}}^{-1}\mathbf{K}_{\Omega_{2,4},\Gamma_{0,1}} \\ -\mathbf{K}_{\Omega_{2,5}}^{-1}\mathbf{K}_{\Omega_{2,5},\Gamma_{0,1}} \\ 0 \\ \mathbf{I}_{n_{0,1}} \end{bmatrix} \quad \begin{bmatrix} 0 \\ 0 \\ -\tilde{\mathbf{K}}_{\Gamma_{1,1}}^{-1}\mathbf{K}_{\Gamma_{1,1},\Gamma_{0,1}} \\ 0 \\ 0 \\ 0 \\ -\tilde{\mathbf{K}}_{\Gamma_{1,2}}^{-1}\mathbf{K}_{\Gamma_{1,2},\Gamma_{0,1}} \\ \mathbf{I}_{n_{0,1}} \end{bmatrix}$$

FIG. 4.5. *The last block column of the three modified block Gaussian eliminators* $\hat{\mathbf{U}}_{\Gamma_{1,1}}$, $\hat{\mathbf{U}}_{\Gamma_{1,2}}$ *and* $\hat{\mathbf{U}}_{\Gamma_{0,1}}$.

Further, suppose that we solve the associated fixed interface eigenvalue problems

$$\mathbf{K}_{\Omega_{\ell,j}}\mathbf{Z}_{\Omega_{\ell,j}} = \mathbf{M}_{\Omega_{\ell,j}}\mathbf{Z}_{\Omega_{\ell,j}}\mathbf{\Lambda}_{\Omega_{\ell,j}}, \quad j = 1, \ldots, s_\ell$$

and coupling mode eigenvalue problems for $i = 0, \ldots, \ell - 1$

$$\tilde{\mathbf{K}}_{\Gamma_{i,j}}\mathbf{Z}_{\Gamma_{i,j}} = \tilde{\mathbf{M}}_{\Gamma_{i,j}}\mathbf{Z}_{\Gamma_{i,j}}\mathbf{\Lambda}_{\Gamma_{i,j}}, \quad j = 1, \ldots, s_i$$

where $\mathbf{Z}_{\Omega_{\ell,j}}^T\mathbf{M}_{\Omega_{\ell,j}}\mathbf{Z}_{\Omega_{\ell,j}} = \mathbf{I}_{n_{\ell,j}}$ and $\mathbf{Z}_{\Gamma_{i,j}}^T\tilde{\mathbf{M}}_{\Gamma_{i,j}}\mathbf{Z}_{\Gamma_{i,j}} = \mathbf{I}_{n_{i,j}}$. Define

$$\mathbf{Z}_\ell = \mathrm{diag}(\mathbf{Z}_{\Omega_{\ell,1}}, \cdots, \mathbf{Z}_{\Gamma_{0,1}}) \tag{4.3}$$

and let

$$\mathbf{R}_\ell = \mathrm{diag}(\mathbf{R}_{\Omega_{\ell,1}}, \cdots, \mathbf{R}_{\Gamma_{0,1}}) \tag{4.4}$$

be the block diagonal matrix of restriction matrices, each with $n_{i,j}$ rows and $m_{i,j} < n_{i,j}$ columns that select the substructure eigenvectors associated with the smallest eigenvalues. As explained in §3, the value of $m_{i,j}$ typically denotes the number of substructure frequencies that lie within a desired frequency range.

Hence, the multilevel extension of Lemma 3.1 results in the reduced eigenvalue problem

$$\hat{\mathbf{D}}\mathbf{x} = \hat{\mathbf{M}}\mathbf{x}\lambda^{m,h} \tag{4.5}$$

where $\hat{\mathbf{D}}$ is a diagonal matrix of order $\sum_{i=0,j=1}^{\ell,s_i} m_{i,j} \equiv m$ and

$$\begin{aligned} (\mathbf{U}_{\ell-1}\mathbf{Z}_\ell\mathbf{R}_\ell)^T\mathbf{K}(\mathbf{U}_{\ell-1}\mathbf{Z}_\ell\mathbf{R}_\ell) &\equiv \hat{\mathbf{D}} \\ (\mathbf{U}_{\ell-1}\mathbf{Z}_\ell\mathbf{R}_\ell)^T\mathbf{M}(\mathbf{U}_{\ell-1}\mathbf{Z}_\ell\mathbf{R}_\ell) &\equiv \hat{\mathbf{M}} \end{aligned}$$

As in §3, we identify $\hat{\mathbf{D}}$ and $\hat{\mathbf{M}}$ as coarse approximations to the stiffness and mass matrices.

In an efficient implementation of AMLS, the computation of the block eliminators are *interleaved* with the computation of the substructure eigenvectors. In other words, the substructure eigenvectors are computed as progress is made towards the root of the tree so that only one pass through $\mathbf{K}$ and $\mathbf{M}$ is necessary. The resulting implementation makes better use of the memory hierarchy. Interleaving, however,

necessitates a modified set of elementary block eliminators $\hat{\mathbf{U}}_{\Gamma_{i,j}}$ for $i = 0, \ldots, \ell - 1$ and $j = 1, \ldots, s_{\ell-1}$. For example, Figure 4.5 shows that the modified eliminators only differ in the last block column.

The reader versed in dense matrix factorizations will recognize the distinction between our two approaches as that between a left-looking and right-looking algorithm for Gaussian elimination. In either case, the result shows that child substructures must be eliminated before parent substructures. The flexibility is that the children within a level may be eliminated in any order and immediately applied to the parents as eliminated. The following result is needed before we state our interleaving result.

LEMMA 4.2. *Let* $i = 0, \ldots, \ell - 1$ *and* $\mathbf{U}_{\Gamma_i} = \Pi_{j=1}^{s_i} \mathbf{U}_{\Gamma_{i,j}}$. *If*

$$\mathbf{U}_{\ell-1} \equiv \mathbf{U}_{\Gamma_{\ell-1}} \mathbf{U}_{\Gamma_{\ell-2}} \cdots \mathbf{U}_{\Gamma_0}$$

then

$$\mathbf{U}_{\ell-1} = \hat{\mathbf{U}}_{\Gamma_{\ell-1}} \hat{\mathbf{U}}_{\Gamma_{\ell-2}} \cdots \hat{\mathbf{U}}_{\Gamma_0} \tag{4.6}$$

where $\hat{\mathbf{U}}_{\Gamma_i} = \Pi_{j=1}^{s_i} \hat{\mathbf{U}}_{\Gamma_{i,j}}$.

Proof. Proof follows from a straightforward induction argument on ℓ. □

We now state and prove our main interleaving result.

THEOREM 4.3. *Let* $\mathbf{Z}_\ell$, $\mathbf{R}_\ell$, $\hat{\mathbf{D}}$, $\hat{\mathbf{M}}$, $\mathbf{U}_{\Gamma_i}$ $\hat{\mathbf{U}}_{\Gamma_i}$, *and* $\mathbf{U}_{\ell-1}$ *be defined by equations (4.3)—(4.5) and Lemma 4.2 and let*

$$\begin{aligned} \mathbf{Z}^e_{\Omega_{\ell,j}} &= \operatorname{diag}(\mathbf{I}_{n_{\ell,1}}, \cdots, \mathbf{Z}_{\Omega_{\ell,j}}, \cdots, \mathbf{I}_{n_{0,1}}) \\ \mathbf{Z}^e_{\Gamma_{i,j}} &= \operatorname{diag}(\mathbf{I}_{n_{\ell,1}}, \cdots, \mathbf{Z}_{\Gamma_{i,j}}, \cdots, \mathbf{I}_{n_{0,1}}) \end{aligned}$$

be matrices of order n *that lift fixed interface and coupling mode eigenvectors. If*

$$\mathbf{Z}_{\Omega_\ell} = \Pi_{j=1}^{s_\ell} \mathbf{Z}^e_{\Omega_{\ell,j}} \quad \text{and} \quad \mathbf{Z}_{\Gamma_i} = \Pi_{j=1}^{s_i} \mathbf{Z}^e_{\Gamma_{i,j}}$$

for $i = 0, \ldots, \ell - 1$ *and* ℓ *a non-negative integer then*

$$\hat{\mathbf{D}} = \mathbf{R}_\ell^T \mathbf{V}_\ell^T \mathbf{K} \mathbf{V}_\ell \mathbf{R}_\ell \quad \text{and} \quad \hat{\mathbf{M}} = \mathbf{R}_\ell^T \mathbf{V}_\ell^T \mathbf{M} \mathbf{V}_\ell \mathbf{R}_\ell \tag{4.7}$$

where

$$\mathbf{V}_\ell = (\hat{\mathbf{U}}_{\Gamma_{\ell-1}} \mathbf{Z}_{\Omega_\ell})(\hat{\mathbf{U}}_{\Gamma_{\ell-2}} \mathbf{Z}_{\Gamma_{\ell-1}}) \cdots (\hat{\mathbf{U}}_{\Gamma_0} \mathbf{Z}_{\Gamma_1}) \mathbf{Z}_{\Gamma_0}$$

Proof. The proof is by induction on ℓ. Lemma 3.1 establishes the base case of $\ell = 1$. Assume that the theorem holds for i levels where i is some positive integer, and $\mathbf{K}$ and $\mathbf{M}$ are ordered corresponding to a nested dissection ordering containing $i+1$ levels. The key result needed before the the inductive hypothesis can be applied is that

$$\hat{\mathbf{U}}_{\Gamma_{i-1}} \cdots \hat{\mathbf{U}}_{\Gamma_0} \mathbf{Z}_{\Omega_{i+1}} = \mathbf{Z}_{\Omega_{i+1}} \hat{\mathbf{U}}_{\Gamma_{i-1}} \cdots \hat{\mathbf{U}}_{\Gamma_0}$$

holds. A simple inductive argument establishes this result; it is simply an observation that $\hat{\mathbf{U}}_{\Gamma_{i-1}} \cdots \hat{\mathbf{U}}_{\Gamma_0}$ is an identity matrix precisely in the locations occupied by the fixed interface eigenvalue problems. Therefore,

$$\begin{aligned} \mathbf{U}_{i+1} \mathbf{Z}_{i+1} &= (\mathbf{U}_{\Gamma_i} \mathbf{U}_{\Gamma_{i-1}} \cdots \mathbf{U}_{\Gamma_0})(\mathbf{Z}_{\Omega_{i+1}} \mathbf{Z}_{\Gamma_i} \cdots \mathbf{Z}_{\Gamma_0}) \\ &= (\hat{\mathbf{U}}_{\Gamma_i} \hat{\mathbf{U}}_{\Gamma_{i-1}} \cdots \hat{\mathbf{U}}_{\Gamma_0})(\mathbf{Z}_{\Omega_{i+1}} \mathbf{Z}_{\Gamma_i} \cdots \mathbf{Z}_{\Gamma_0}) \\ &= (\hat{\mathbf{U}}_{\Gamma_i} \mathbf{Z}_{\Omega_{i+1}})(\hat{\mathbf{U}}_{\Gamma_{i-1}} \cdots \hat{\mathbf{U}}_{\Gamma_0})(\mathbf{Z}_{\Gamma_i} \mathbf{Z}_{\Gamma_{i-1}} \cdots \mathbf{Z}_{\Gamma_0}) \\ &= (\hat{\mathbf{U}}_{\Gamma_i} \mathbf{Z}_{\Omega_{i+1}}) \mathbf{V}_i \\ &= \mathbf{V}_{i+1} \end{aligned}$$

$$\hat{\mathbf{D}} = \begin{bmatrix} \mathbf{\Lambda}_{m_{2,1}} & 0 & 0 & 0 & 0 & 0 & 0 & 0 \\ & \mathbf{\Lambda}_{m_{2,2}} & 0 & 0 & 0 & 0 & 0 & 0 \\ & & \mathbf{\Lambda}_{m_{1,1}} & 0 & 0 & 0 & 0 & 0 \\ & & & \mathbf{\Lambda}_{m_{2,3}} & 0 & 0 & 0 & 0 \\ & & & & \mathbf{\Lambda}_{m_{2,4}} & 0 & 0 & 0 \\ & & & & & \mathbf{\Lambda}_{m_{2,5}} & 0 & 0 \\ & & & & & & \mathbf{\Lambda}_{m_{1,2}} & 0 \\ & & & & & & & \mathbf{\Lambda}_{m_{0,1}} \end{bmatrix}$$

FIG. 4.6. *The final stiffness matrix*

where the second equality follows from Lemma 4.2, the third equality because there are no fixed interface eigenvalue problems on level i and so $\mathbf{Z}_{\Omega_i} = \mathbf{I}$ and the final equality uses our inductive hypothesis. The conclusion of the theorem now easily follows. □

Equation (4.7) states that after the initial block Gaussian eliminators for level $\ell - 1$ are applied, the solutions of the fixed interface eigenvalue problems are applied as a congruence transformation. The remainder of the process is a sequence of modified block Gaussian eliminators followed by the coupling mode eigenvectors applied as a congruence transformation. Finally, restrictions are applied that retain only substructure eigenvalues and eigenvectors that lie in the desired frequency range of interest.

Theorem 4.3 demonstrates how the interleaving is accomplished; however, in practice, the restrictions are not delayed. Instead, the restrictions are applied by only computing partial solutions of all the fixed interface and coupling mode eigenvalue problems and only these eigenvectors are applied during the congruence transformation. For example, a Lanczos based eigensolver may be used for these partial eigensolutions. This dramatically reduces the cost associated with the various eigenvalue problems. (The restrictions were not interleaved purely for the complexity in notation introduced.) We refer the reader to the recent thesis [10] of Kaplan for details on a high quality and efficient implementation of AMLS applied to the numerical solution of frequency response problems. The next section will give examples of how the size of the partial eigenvalue problem is determined in practical computation.

The interleaving of the restrictions implies that the size of the transformed stiffness and mass matrices decreases as interleaving progresses. Figures 4.6 and 4.7 display the final stiffness and mass matrices.

5. Numerical Experiments. In this section we present two examples. The first example applies AMLS to determine the free vibrations of a membrane. The goal of the first example to understand the eigenvalue and eigenvector approximations computed by AMLS and the interplay between the FEM discretization and modal truncation errors. The second example presents AMLS applied to determine the frequencies and modes of an automobile body. The goal of the second example to give an indication of the efficiency of AMLS on a large-scale industrial example.

5.1. Free Vibrations of a Membrane. We apply AMLS to the differential eigenvalue problem associated with a membrane on the unit square. The eigenvalue

$$\hat{\mathbf{M}} = \begin{bmatrix} \mathbf{I}_{m_{2,1}} & 0 & \check{\mathbf{M}}_{\Omega_{2,1},\Gamma_{1,1}} & 0 & 0 & 0 & 0 & \check{\mathbf{M}}_{\Omega_{2,1},\Gamma_{0,1}} \\ & \mathbf{I}_{m_{2,2}} & \check{\mathbf{M}}_{\Omega_{2,2},\Gamma_{1,1}} & 0 & 0 & 0 & 0 & \check{\mathbf{M}}_{\Omega_{2,2},\Gamma_{0,1}} \\ & & \mathbf{I}_{m_{1,1}} & 0 & 0 & 0 & 0 & \check{\mathbf{M}}_{\Gamma_{1,1},\Gamma_{0,1}} \\ & & & \mathbf{I}_{m_{2,3}} & 0 & 0 & \check{\mathbf{M}}_{\Omega_{2,3},\Gamma_{1,2}} & \check{\mathbf{M}}_{\Omega_{2,3},\Gamma_{0,1}} \\ & & & & \mathbf{I}_{m_{2,4}} & 0 & \check{\mathbf{M}}_{\Omega_{2,4},\Gamma_{1,2}} & \check{\mathbf{M}}_{\Omega_{2,4},\Gamma_{0,1}} \\ & & & & & \mathbf{I}_{m_{2,5}} & \check{\mathbf{M}}_{\Omega_{2,5},\Gamma_{1,2}} & \check{\mathbf{M}}_{\Omega_{2,5},\Gamma_{0,1}} \\ & & & & & & \mathbf{I}_{m_{1,2}} & \check{\mathbf{M}}_{\Gamma_{1,2},\Gamma_{0,1}} \\ & & & & & & & \mathbf{I}_{m_{0,1}} \end{bmatrix}$$

FIG. 4.7. *The final mass matrix*

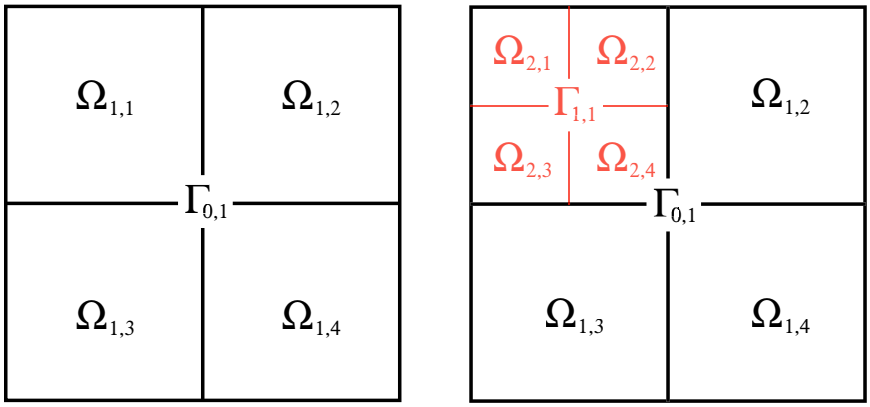

FIG. 5.1. *The recursively partitioned to level $\ell = 2$ unit square. All of the subdomains $\Omega_{1,j}$ for $j = 2, 3, 4$ are also partitioned as $\Omega_{1,1}$.*

problem in strong form is

$$-\Delta u = \lambda u \tag{5.1}$$

with Dirichlet boundary conditions on all four edges. The eigenvalues for (5.1) are given by $\lambda_{i,j} = \pi^2(i^2 + j^2)$ and so the frequencies are given by

$$\omega_{i,j} = \frac{\sqrt{\lambda_{i,j}}}{2\pi} = \frac{\sqrt{i^2 + j^2}}{2}$$

for i and j positive integers. We are interested in determining dimensionless frequencies up through 4 ($\omega_{i,j} \leq 4$) and corresponding eigenvectors. A finite element discretization using a uniform triangulation with bilinear elements generates stiffness and mass matrices $\mathbf{K}$ and $\mathbf{M}$. AMLS is then applied to compute approximations to the eigenvalues and eigenvectors of the matrix pencil $(\mathbf{K}, \mathbf{M})$.

Figures 5.2—5.5 give the relative errors with respect to the exact eigenvalues, for a given FEM discretization, as computed by a Matlab implementation of AMLS and the Matlab routine `eigs`. Before commenting on the Figures, we provide some details on the two Matlab routines.

The Matlab routine `eigs` solves the generalized eigenvalue problem corresponding to the matrix pencil $(\mathbf{K}, \mathbf{M})$ by computing the eigenvalues of the shift-invert (with

TABLE 5.1

The orders of the substructures. The top row displays the global matrix order. Notation from §4 is used in order to indicate various parameters. Note that because all the substructures at a level are equivalent, $n_{i,1} = \cdots = n_{i,s_i}$.

	2,209	9,025	36,481	57,121
ℓ	2	3	4	4
$n_{0,1}(s_0)$	93 (1)	189 (1)	381 (1)	477 (1)
$n_{1,j}(s_1)$	45 (4)	93 (4)	189 (4)	237(4)
$n_{2,j}(s_2)$	121 (16)	45 (16)	93 (16)	117 (16)
$n_{3,j}(s_3)$		121 (64)	45 (64)	57 (64)
$n_{4,j}(s_4)$			121 (256)	196 (256)

TABLE 5.2

The number of modes retained and the frequency cut-off used for all the substructure eigenvalue problems. The top row displays the global matrix order. Notation from §4 is used in order to indicate various parameters. In particular, m denotes the total number of substructure modes retained (the order of the final eigenvalue problem (4.5)) so determining the approximations to the free vibrations of the membrane. Note that because all the substructures at a level are equivalent, $m_{i,1} = \cdots = m_{i,s_i}$.

	2,209	9,025	36,481	57,121
$m_{0,1}$ (freq. cut-off)	13 (5.0)	13 (5.0)	13 (5.0)	13 (5.0)
$m_{1,j}$ (freq. cut-off)	9 (7.9)	9 (7.9)	9 (7.9)	9 (7.9)
$m_{2,j}$ (freq. cut-off)	8 (7.9)	7 (11.9)	7 (11.9)	7 (11.8)
$m_{3,j}$ (freq. cut-off)		4 (11.9)	5 (17.2)	5 (17.1)
$m_{4,j}$ (freq. cut-off)			1 (17.2)	1 (17.1)
m	177	417	737	737

shift set to zero) system

$$\mathbf{K}^{-1}\mathbf{M}\mathbf{x} = \frac{1}{\lambda}\mathbf{x}$$

by using the appropriate ARPACK [13] subroutine. The subroutine implements an implicitly restarted Lanczos method. The Matlab sparse Cholesky solver is used for solving the necessary linear systems. We refer the reader to the online Matlab documentation of `eigs` for further details. All the Lanczos runs are computed in this fashion. We set the tolerance for `eigs` equal to machine precision and computed frequencies up through 5. We comment that although the resulting residuals (measured using a discrete L_2 norm) were of order machine precision, the finite element discretization error is substantially larger. Hence, we can regard the eigenvalues and eigenvectors as computed by `eigs` as accurate as allowed by the finite element discretization, and these represent an accuracy benchmark for comparing against AMLS.

The Matlab routine implementing AMLS for the membrane problem partitions the domain $\Omega_{0,1}$ into four subdomains $\Omega_{1,i}$ by the cross-shaped interface $\Gamma_{0,1}$; each subdomain is recursively partitioned to ℓ levels in a similar fashion. Figure 5.1 illustrates the process for $\ell = 2$ levels. Therefore, the number of substructures on level i is simply $s_i = 4^i$. Tables 5.1 and 5.2 list, for each membrane problem for which results are presented, the order of the global problem, the number of levels ℓ, the order and number of fixed-interface eigenvalue problems, the order and number of coupling mode eigenvalue problems for each level, the number of retained modes for each substructure and the order of the final eigenvalue problem (4.5). The block

Gaussian eliminators are computed by using the Matlab sparse Cholesky solver. The fixed interface and coupling mode eigenvalue problems were solved by using the Matlab routine `eig` (no `s` appended). The eigenvalue problem (4.5) is solved by a call to `eigs` to compute all the eigenvalues and corresponding eigenvectors through 4 . Finally, we obtain approximations to the eigenvectors of the matrix pencil $(\mathbf{K}, \mathbf{M})$ by premultiplying the eigenvectors of (4.5) by $\mathbf{V}_\ell \mathbf{R}_\ell$.

We now return to a discussion of Figures 5.2—5.5. These figures display plots of the relative errors for the eigenvalues as computed by AMLS and `eigs`. Recall that the error for the AMLS computed eigenvalues is associated with both the finite element discretization and the AMLS mode truncation. The figures show that the error associated with mode truncation can be nearly as small as that of the discretization error. Figures 5.2—5.4 also demonstrate that the eigenvalues computed by AMLS achieve nearly the quadratic rate of convergence inherent in the finite element discretization. Figure 5.5, in particular shows that the number m of substructure modes retained does not increase even though the order of the global problem increased from $36,481$ to $57,121$.

Finally, Figures 5.6—5.7 plot information concerning the quality of the computed eigenvectors. Figure 5.6 displays the sines of the angles between the eigenspace as computed by `eigs` and AMLS up through 4 for matrix orders $2,209$, $9,025$ and $36,481$. Given our earlier comments concerning the accuracy of the eigenvalues and eigenvectors as computed by the Lanczos routine `eigs`, AMLS computes eigenvectors that are nearly as accurate as allowed by the finite element discretization. Figure 5.7 displays the discrete L_2 residual errors of the eigenvalues and eigenvectors as computed by AMLS for matrix orders $2,209$, $9,025$ and $36,481$.

5.2. Automobile Body. For an example of the application of AMLS to industrial problems, we briefly present results for the analysis of a automobile body [1]. A finite element discretization of dimension 2.9 million was generated for this vehicle body at an automobile company. Using the MSC.Nastran commercial version of the Lanczos eigensolver implementation described in [7], we determined that there were 824 eigenpairs with natural frequencies up to 400 .

To approximate these eigenpairs using AMLS, we generated a substructure tree automatically based on the sparsity of the stiffness and mass matrices, having $12,068$ substructures on 24 levels. We obtain partial eigensolutions for substructures with a frequency cut-off of 4000 on all levels, yielding a total of $m = 40,336$ substructure eigenvectors. Table 5.3 presents the accuracy of the AMLS approximate natural frequencies relative to the Lanczos results. With AMLS, this problem can be solved on one workstation processor (200 Mhz IBM RISC) in about half the time required for solution on a multiprocessor vector supercomputer (a Cray T90) using the commercial Lanczos implementation. We are not aware of a calculation similar in scope computed on a low-end workstation.

6. Conclusions. In this report we presented the automated multilevel substructuring (AMLS) method for approximating eigenpairs in elastodynamics. This was accomplished by dividing the problem domain recursively into subdomains on multiple levels. We then generated an approximating subspace by obtaining eigenfunctions associated with subdomains and the interfaces between them.

We first examined the method in the continuous setting. We solve fixed-interface eigenvalue problems on subdomains and interfaces where the Steklov-Poincaré operator represents elastic behavior and a new interface mass operator was defined to represent inertial effects consistently. All of these eigenvalue problems were shown to

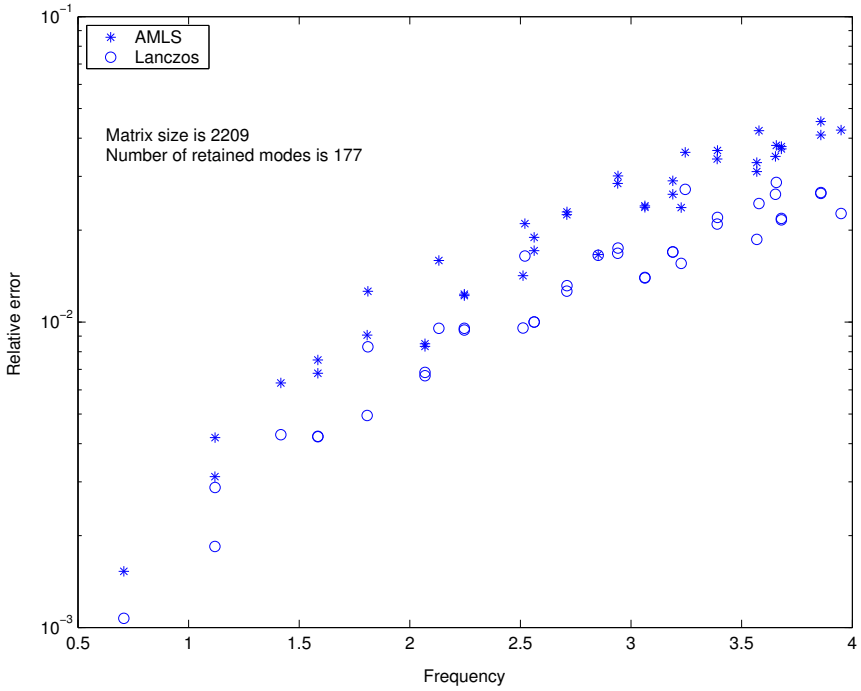

FIG. 5.2. *Comparing relative errors in the eigenvalues as computed by AMLS and Lanczos: Matrix size of 2,209.*

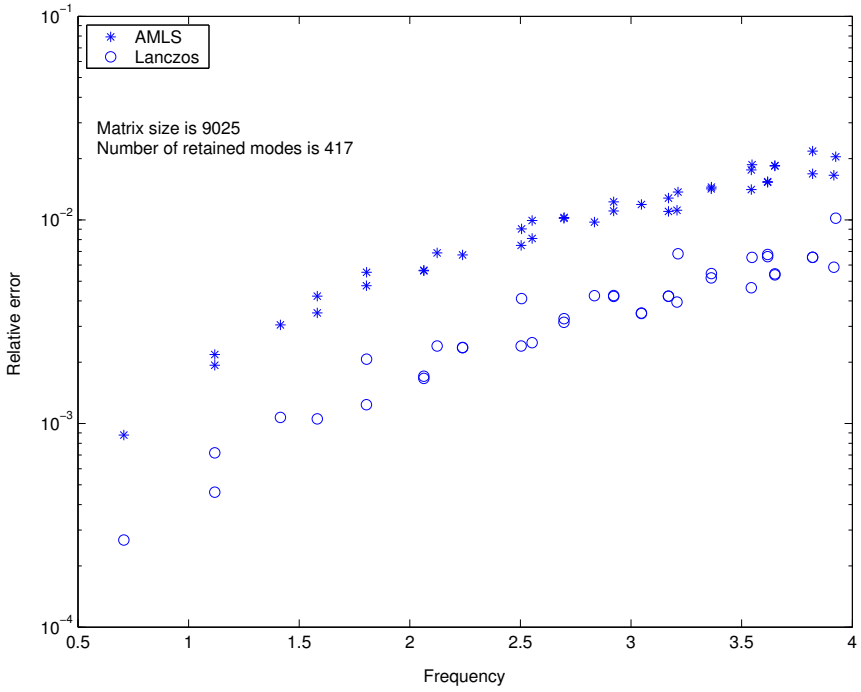

FIG. 5.3. *Comparing relative errors in the eigenvalues as computed by AMLS and Lanczos: Matrix size of 9,025.*

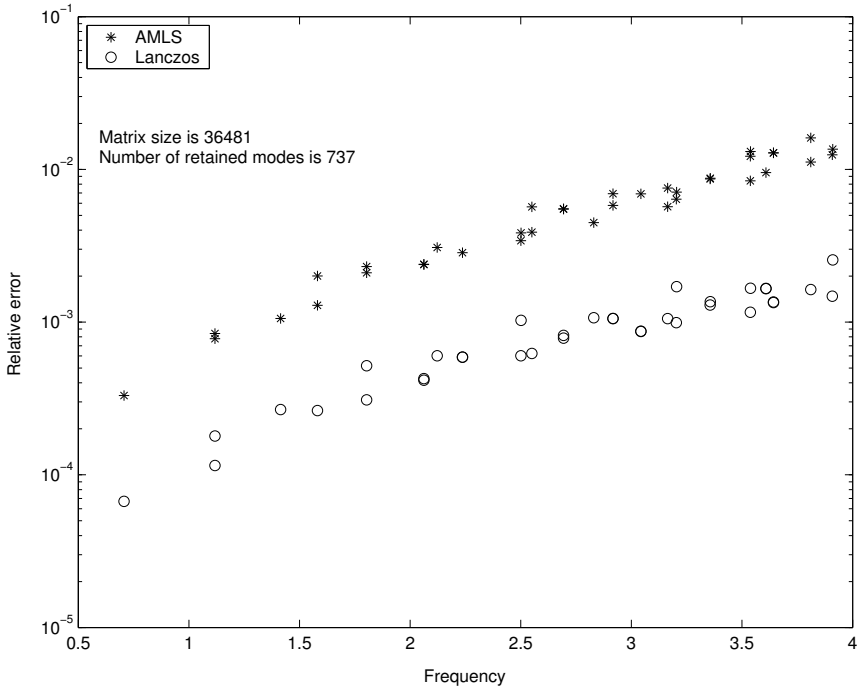

FIG. 5.4. *Comparing relative errors in the eigenvalues as computed by AMLS and Lanczos: Matrix size of 36,481.*

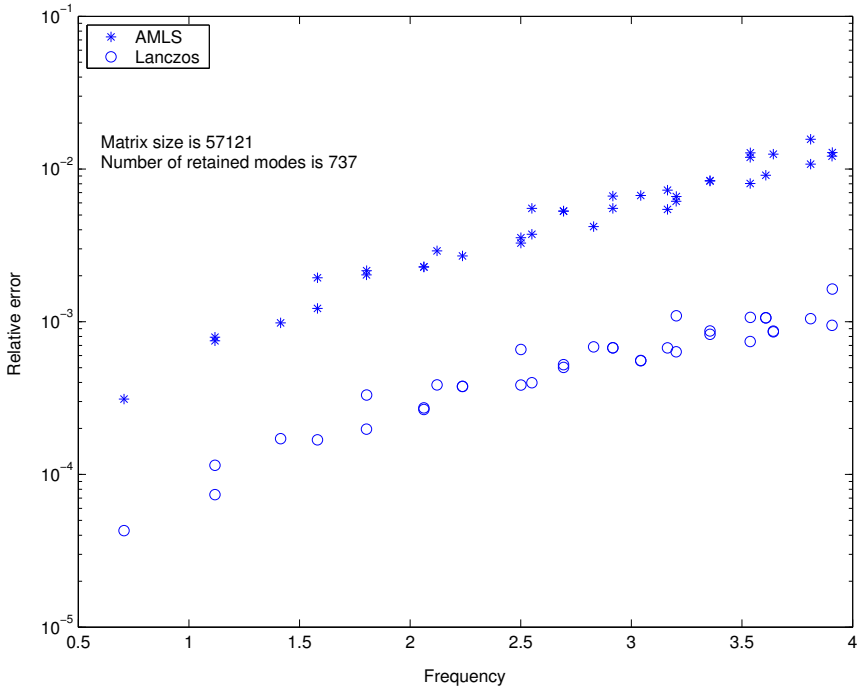

FIG. 5.5. *Comparing relative errors in the eigenvalues as computed by AMLS and Lanczos: Matrix size of 57,121.*

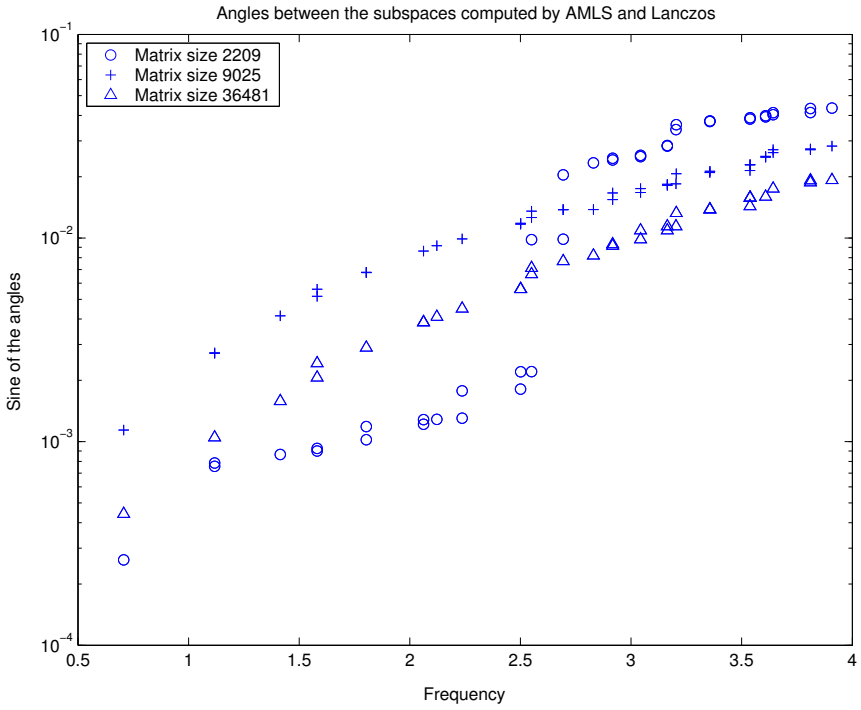

FIG. 5.6. *Angles between the subspaces.*

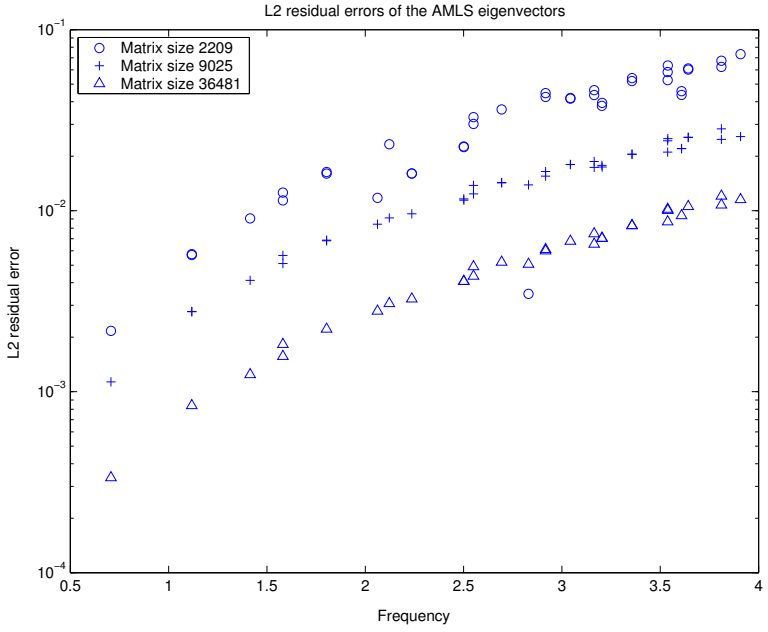

FIG. 5.7. *L_2 residual errors of the approximate eigenvalues and eigenvectors as computed by AMLS.*

TABLE 5.3
Industrial example: accuracy of natural frequencies

Frequency range	Relative accuracy of natural frequencies	Number of natural frequencies in range
0-50	< 0.00003	18
50-100	< 0.00015	40
100-200	< 0.0005	164
200-300	< 0.0013	266
300-400	< 0.003	336

be projections of the global eigenvalue problem onto a hierarchy of subspaces that are orthogonal in the energy inner product. The error associated with truncating these subspaces in the continuous setting is mesh-independent. We remark that although we presented AMLS for linear elastodynamics, our formulation is abstract and applies to generic H^1-elliptic bilinear forms.

We showed that AMLS is a generalization of classical component mode synthesis (CMS) techniques. In particular, our variational formulation is a multilevel extension of work by Bourquin, and Bourquin and d'Hennezel [2, 3, 5, 4] that contains the first mathematical analysis of CMS. In addition, we proved that AMLS is a congruence transformation that arises from a matrix decomposition of the stiffness matrix. The congruence transformation was carefully linked to the variational formulation of AMLS. This congruence transformation allows us to treat AMLS as a purely algebraic process. To the best of knowledge, our report is the first study that investigates multilevel substructuring for elliptic PDE eigenvalue problems; the breakthrough calculations in the paper by Kropp and Heiserer achieved by AMLS justifies a careful description of the underlying algorithm [12].

Acknowledgments. We wish to thank Matt Kaplan for the various diagrams in the report and many useful discussions; Pavel Bochev for reading through an early draft; Olof Widlund for pointing out the work of Bourquin to the second author; Leszek Demkowicz for various useful comments on trace spaces; Ulrich Hetmaniuk for a careful reading of our original submission; Frderic Bourquin, John Lewis and Bruce Hendrickson for helpful discussion; and finally the referees and editor for suggestions that led to the improvement of the initial submission.

REFERENCES

[1] J. K. BENNIGHOF, M. F. KAPLAN, AND M. B. MULLER, *Extending the frequency response capabilities of automated multi-level substructuring*, no. AIAA-2000-1574, April 2000.

[2] F. BOURQUIN, *Analysis and comparison of several component mode synthesis methods on one-dimensional domains*, Numerische Mathematik, 58 (1990), pp. 11–34.

[3] ———, *Component mode synthesis and eigenvalues of second order operators: Discretization and algorithm*, Mathematical Modeling and Numerical Analysis, 26 (1992), pp. 385–423.

[4] F. BOURQUIN AND F. D'HENNEZEL, *Intrinsic component mode synthesis and plate vibrations*, Computers and Structures, 44 (1992), pp. 315–324.

[5] ———, *Numerical study of an intrinsic component mode synthesis method*, Computer Methods in Applied Mechanics and Engineering, 97 (1992), pp. 49–76.

[6] R. R. CRAIG, JR. AND M. C. C. BAMPTON, *Coupling of substructures for dynamic analysis*, AIAA Journal, 6 (1968), pp. 1313–1319.

[7] R. G. GRIMES, J. G. LEWIS, AND H. D. SIMON, *A shifted block Lanczos algorithm for solving sparse symmetric generalized eigenproblems*, SIAM J. Matrix Analysis and Applications, 15 (1994), pp. 228–272.

[8] B. Hendrickson and R. Leland, *The Chaco user's guide: Version 2.0*, Tech. Report SAND94–2692, Sandia National Labs, Albuquerque, NM, June 1995.

[9] W. C. Hurty, *Vibrations of structural systems by component-mode synthesis*, Journal of the Engineering Mechanics Division, ASCE, 86 (1960), pp. 51–69.

[10] M. F. Kaplan, *Implementation of Automated Multilevel Substructuring for Frequency Response Analysis of Structures*, PhD thesis, The University of Texas at Austin, Department of Aerospace Engineering & Engineering Mechanics, Austin, TX, 2001.

[11] G. Karypis and V. Kumar, *A fast and high quality multilevel scheme for partitioning irregular graphs*, Tech. Report CORR 95–035, University of Minnesota, Dept. Computer Science, Minneapolis, MN, June 1995.

[12] A. Kropp and D. Heiserer, *Efficient broadband vibro-accoustic analysis of passenger car bodies using an FE-based component mode synthesis approach*, in Proceedings of the Fifth World Congress on Computational Mechanics (WCCM V) July 7-12, H. A. Mang, F. G. Rammerstorfer, and J. Eberhardsteiner, eds., Austria, 2002, Vienna University of Technology. ISBN 3-9501554-0-6 (http://wccm.tuwien.ac.at).

[13] R. B. Lehoucq, D. C. Sorensen, and C. Yang, *ARPACK USERS GUIDE: Solution of Large Scale Eigenvalue Problems with Implicitly Restarted Arnoldi Methods*, SIAM, Phildelphia, PA, 1998.

[14] A. Quarteroni and A. Valli, *Domain Decomposition Methods for Partial Differential Equations*, Numerical Mathematics and Scientific Computation, Oxford University Press, Oxford, UK, first ed., 1999.

[15] P. Seshu, *Substructuring and component mode synthesis*, Shock and Vibration, 4 (1997), pp. 199–210.